Polymer Photovoltaic Devices Fabricated with Blend MEHPPV and Organic Small Molecules

Xianyu Deng,[†] Liping Zheng,[†] Chunhe Yang,[‡] Yongfang Li,[‡] Gang Yu,*[,§] and Yong Cao*[,†]

Institute of Polymer Optoelectronic Materials and Devices, South China University of Technology, Guangzhou, 510640, P.R.China, Institute of Chemistry, Chinese Academy of Sciences, Beijing 100080, P.R. China

Received: September 5, 2003; In Final Form: January 6, 2004

A series of commercial organic materials was blended into MEHPPV (poly[2-methoxy, 5-(2-ethylhexoxy)-1,4-phenylene vinylene]) and used as electron acceptors in the polymer heterojunction photovoltaic cells and photodiodes. Electrochemical cyclic voltammetry (CV) was used to determine the acceptors' lowest unoccupied molecule orbit (LUMO) levels. We demonstrated that the LUMO of the acceptor had remarkable effect on the open-circuit voltage for the donor and acceptor composite devices over ∼1 eV range at LUMO near 4.0 eV. The photoresponse can be further enhanced by the substitution of a long alkyl chain in the polar acceptor molecules. For device with the substituted acceptor doped into MEHPPV as an active layer, its photosensitivity at zero bias is increased by a factor of 4−0.00047 A/W in comparison with 0.00012 A/W for unsubstituted acceptor. At a voltage of −30 V, the photosensitivity reaches 0.14 A/W, the same level as for device from MEHPPV: PCBM at 0 V bias. A strong electric field and temperature dependence in the composite devices was also observed and discussed.

I. Introduction

Organic semiconductors are currently regarded as a promising candidate for applications in the field of energy conversion, such as large-area photodetectors[1,2] and solar cells.[3,4] For photovoltaic cells (PVCs) made from pure conjugated polymers, energy conversion efficiencies were typically in the range of $10^{-3}-10^{-2}$ %,[5−7] too low to be used in practical applications. The discovery of fast photoinduced electron transfer at the interface between a semiconductor polymer and buckminsterfullerene, C_{60} and its derivatives,[5,8] provided a molecular approach to improve carrier generation and collection efficiency. Photocurrents in conjugated polymer MEHPPV films were enhanced by introducing fullerene molecules as the sensitizers for high efficiency solar cells and high sensitivity photodetectors.[9] Charge transfer (CT) and subsequent charge separation occur in the charges generated by photoexcitation: the photoinduced electrons favor energetically moving into the C_{60} phase with larger electron affinity (acceptor phase, A) while the photoinduced holes favor energetically moving into the polymer phase with smaller ionization potential (donor phase, D). The photoinduced CT separates electrons and holes and protects them from early time recombination. By controlling the morphology of the phase separation into an interpenetrating bi-continuous network of D and A phases, one can achieve a high interfacial area within a "bulk D/A heterojunction" material.[4,10] Moreover, a bi-continuous network can provide the needed pathways for collecting the separated carriers at the external electrodes: holes from the donor phase and electrons from the acceptor phase. Thus, thin film sandwich devices with a bi-continuous D/A composite as the active material can function as efficient photovoltaic cells and efficient photodetectors with high carrier collection efficiency.[4,11] High-performance photosensors in the metal/polymer/metal configuration have been demonstrated with external quantum efficiency (EQE) close to 100% el/ph.[2,4] In the earlier publications,[12] the photosensitivity of polymer PVCs made from MEHPPV:PCBM blends reached 0.1−0.15 A/Watt, equivalent to quantum efficiency of 30−45% (el/ph), while the energy conversion efficiency reached over 3.0% (500 nm, 10 mW/cm^2). Recent reports are concentrated on improving the composite D/A phase[13,14] and interfacial structure of polymer/electrode,[15,16] selecting novel conjugated polymers to match the LUMO level of acceptors[17] and looking for conjugated polymers with better match-up of the terrestrial solar spectrum[18] and with higher charge mobility.[19] Shaheen et al.[20] reported a great influence of solvent on the D/A phase behavior and the device performance. Brabec et al. synthesized a series of soluble fullerene derivatives with LUMO energy varied in ∼0.2 eV range and found out that the open-circuit voltage of the corresponding devices are directly correlated with the acceptor strength of these fullerenes.[10] They concluded that the Fermi level of the negative electrode metal was pinned to the LUMO of the fullerenes. The energy conversion efficiency of polymer solar cells have now reached 2.5% under AM1.5 solar conditions (80 mW/cm^2).[20,21]

Nevertheless, the energy conversion efficiency and the photosensitivity of the polymer photovoltaic devices are still too low for practical application. To obtain better understanding of how acceptor phase affects the device performance and improves the efficiency and the photosensitivity of polymer PVCs, in this paper, a series of organic molecules with wide range of acceptor strengths was doped into conjugated polymer MEHPPV and was used as an active layer for the fabrication of polymer PVCs. The open-circuit voltage was strongly

* Corresponding authors. E-mail: poycao@scut.edu.cn, gangyu@dupontdisplays.com.
[†] South China University of Technology.
[‡] Chinese Academy of Sciences.
[§] Permanent address: DupontDisplays, 600 Ward Drive, Santa Barbara, CA 93111.

10.1021/jp036649i CCC: $27.50
Published on Web 02/20/2004

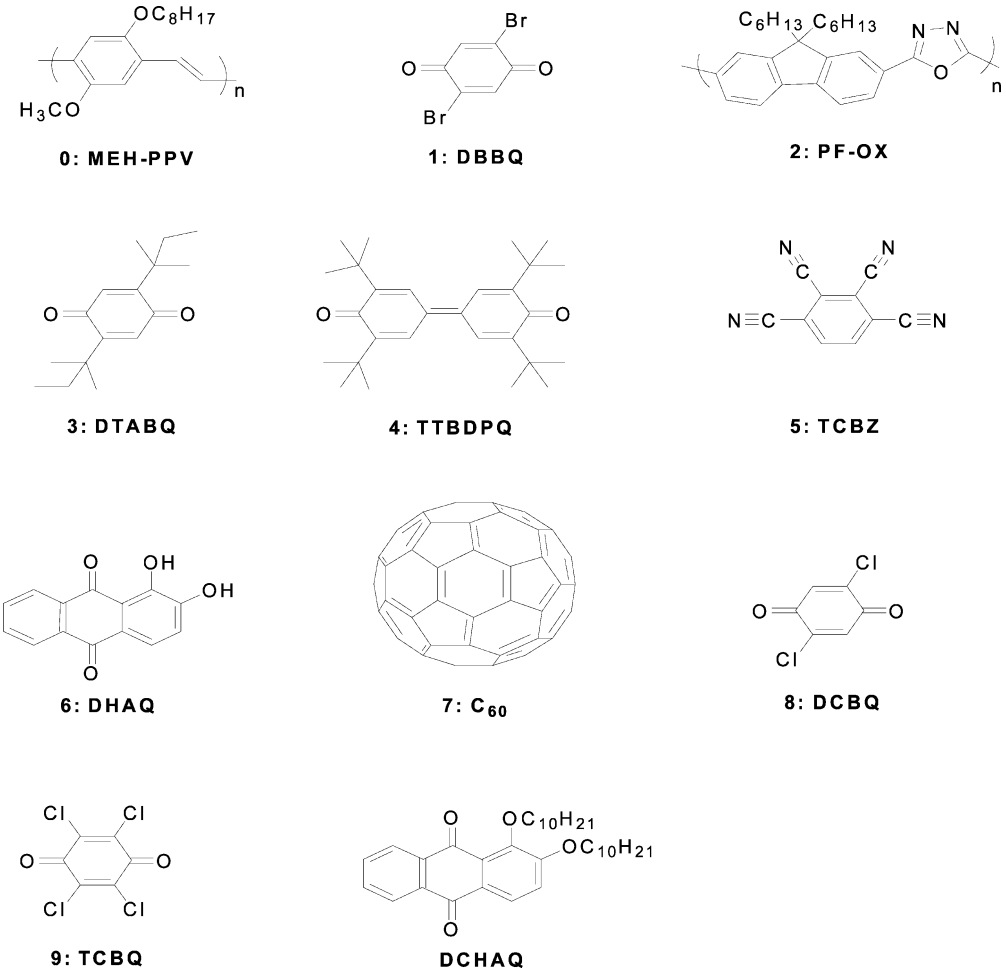

Figure 1. Chemical structure of the organic molecules.

dependent on the LUMO level of acceptors in the range of almost 1 eV. Attaching a long alkoxy chain into core of small organic acceptor significantly improves device efficiency. This indicates that both the compatibility of acceptor phase with polymer donor phase and mobility are important to device performance.

II. Experimental Section

Fullerene C_{60} was purchased from Tianan Comp. 7-(9,9′-Dihexyl-fluorene)-oxadiazole-copolymer (PF−OX) was synthesized according to ref 22. MEHPPV was synthesized following the procedure described by F. Wudl's group.[23] Organic acceptor molecules were purchased from TCI and Aldrich. The structure of acceptors used in this study are listed in Figure 1.

Commercial acceptors were investigated by electrochemical cyclic voltammetry (CV). The electrochemical measurements of the organic molecules were performed in an electrolyte consisting of 0.1 mol/L tetrabutylammonium hexafluorophosphate ($TBAPF_6$) dissolved in an acetonitrile solution. In each case, a glassy carbon was used as the working electrode, platinum wire was used as a counter electrode, and saturated calomel electrode was used as a quasi-reference electrode. All the preparation steps and experiments were carried out in a controlled atmosphere drybox under nitrogen. LUMO levels were determined from onset of n-doping by the empirical formula ($E_{LUMO} = -e(E_{red} + 4.4)$ (eV).[24] The photoluminescent (PL) efficiency measurement was carried out with an integrating sphere (IS-080, Labsphere) combined with a Si photodetector with flat photoresponse from 300 nm to 800 nm. A 488-nm line of argon ion laser was used as an excitation source. The PL spectra were recorded with a CCD spectrophotometer (Instaspec 4, Oriel Co.). The absorption spectrum was taken by HP 8453 spectrophotometer.

The typical device structure used in this study was a sandwich structure with ITO/PEDOT as a hole-collecting electrode and Ba/Al as an electron-collecting electrode. A 50-nm-thick poly(ethylene dioxythiophene)/polystyrenesulfonic acid (PEDT-PSS, Batron-P, Bayer AG) layer was spin-coated on the top of ITO along with an active layer to reduce the device leakage. The molecular acceptors were dissolved in a *p*-xylene or THF solution. MEHPPV was dissolved in a solution with THF/*p*-xylene (2:8). Both solutions were mixed to give the weight ratio of donor material to acceptor material of 3:1. The blend solution was spin-coated on the top of PEDT-PSS layer, resulting in 100-nm active layer. The thickness was determined by the surface profilometer (ALFA-Step 500, Tencor). Finally, 3−5 nm of barium followed by 150-nm-thick Al layers were thermally evaporated on the top of the photoactive polymer blend. The deposition rates and the thickness of the evaporation layers were monitored by a thickness/rate meter (Sycon). The deposition rates of barium and aluminum were, respectively, 0.1−0.2 A/s and 1−2 nm/s. The overlap area between the cathode and the anode define the device active area. Other than described specifically, 0.15 cm^2 active area was typically used in this study. All the fabrication steps, except spin-casting PEDT:PSS layer, were carried out in a nitrogen

TABLE 1: PL and LUMO of MEH−PPV Doped with Organic Molecule (Weight ratio of acceptor to MEHPPV equal 1:3)

	MEHPPV (pure)	DBBQ (1)	PF-OX (2)	DTABQ (3)	TTBDPQ (4)	TCBZ (5)	DHAQ (6)	C60 (7)	DCBQ (8)	TCBQ (9)
LUMO (eV)		3.44	3.60	3.62	3.74	3.79	3.82	3.84	4.08	4.40
PL (%)	19.8	2.02	8.07	11.1	6.24	0.10	2.65	2.59	9.81	2.16

glovebox. The IV characteristics in dark and under illumination were measured with a Keithley 236 source-measure unit. Photocurrent was measured under illumination (10 mW/cm^2, 500 nm) by means of a tungsten lamp. The action spectrum was measured with a commercial photomodulation spectroscopic setup including a xenon lamp, an optical chopper, a monochromator, and lock-in amplifier operated by PC computer (Merlin, Oriel). A calibrated Si photodiode was used as a standard for the determination of photosensitivity.

The energy conversion efficiency η_e and fill-factor (FF) were calculated by the following equations:[13]

$$\eta_e = \mathrm{FF} \times I_{sc} \times V_{oc}/P_{in} \quad (1)$$

and

$$\mathrm{FF} = I_m V_m / I_{sc} V_{oc} \quad (2)$$

where P_{in} is the incident radiation flux, I_{sc} and V_{oc} are short-circuit current and open-circuit voltage, and I_m and V_m are current and voltage under maximum power condition.

III. Results and Discussion

The redox properties were investigated by a cyclic voltammogram. Table 1 summarizes LUMO level derived from the onset in the cyclic voltammograms of the acceptor molecules. The weak organic acceptors for this study were chosen on the basis of the LUMO levels which are close to the LUMO level of C_{60} (3.84 eV). These acceptors show a variation of LUMO levels about ±0.5 eV above and below C_{60} LUMO level (from 3.44 eV for DBBQ to 4.40 eV for TCBQ). According to the LUMO level values, all of the organic molecules were numbered from low to high as follows: (1) 2,5-dibromo-1,4-benzoquinone (DBBQ); (2) 2,7-(9,9′-dihexyl-fluorene)-oxadiazole-copolymer (PF-OX); (3) 2,5-di-*tert*-amylbenzoquinone (DTABQ); (4) 3,3′,5,5′-tetra-*tert*-butyl-4,4′-diphenzoquinone (TTBDPQ); (5) 1,2,4,5-tetracyanobenzene (TCBZ); (6) 1,2-dihydroxyanthraquinone (DHAQ); (7) C_{60}; (8) 2,5-dichloro-1,4-benzoquinone (DCBQ); (9) tetrachloro-1,4-benzoquinone (TCBQ). The interaction between the organic molecules and MEHPPV was investigated by means of PL quenching measurements. Absolute PL efficiency was measured for pristine MEHPPV and blend films. Results are included in Table 1, from which it is seen that the PL emission of MEHPPV was remarkably quenched for MEHPPV films blended with the organic molecule acceptors (including C_{60}). Since the LUMO levels of these organic acceptors are substantially lower than the LUMO of MEHPPV, the electron affinity of these organic molecules is significantly greater than that of MEHPPV. Thus, one can anticipate that photoinduced electrons on MEHPPV chains will energetically favor transfer onto organic molecules in MEHPPV/acceptor composites. This is consistent with the PL quenching in these blends. The degree of PL quenching is not correlated with the LUMO level of acceptor molecule. Acceptors PF-OX (2), DTABQ (3), and DCBQ (8) show much less quenching. We speculate that it may be due to the aggregation of acceptor molecules in the blend.

Figure 2 shows the current−voltage response of the devices, measured under illumination of a broad-band white light. Device

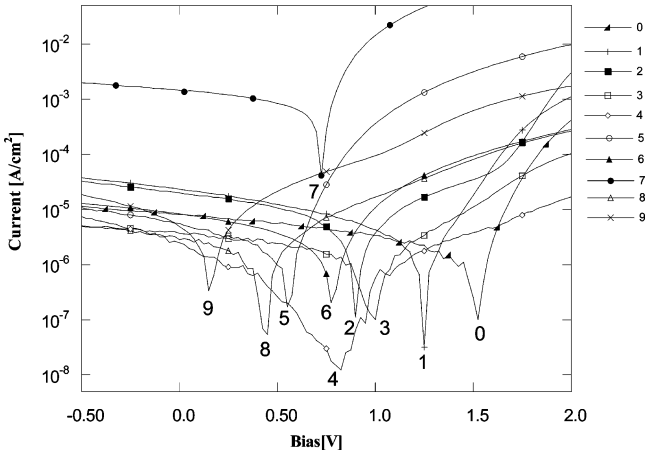

Figure 2. I−V characteristics of devices made with MEHPPV doped with organic molecule under white light illumination (10 mW/cm^2): 0: MEHPPV, 1: MEHPPV/DBBQ; 2: MEHPPV/PF-OX; 3: MEHPPV/DTABQ; 4: MEHPPV/ TTBDPQ, 5: MEHPPV/TCBZ, 6: MEHPPV/DHAQ, 7: MEHPPV/C_{60}, 8: MEHPPV/DCBQ, 9: MEHPPV/TCBQ.

with pure MEHPPV was also fabricated as a reference. From Figure 2, the open-circuit voltage (V_{oc}) of the device with pure MEHPPV is 1.5 V, which is consistent with the results reported previously for devices with Ca cathode.[25] The devices from MEHPPV blended with the acceptor result in significant reduction of V_{oc}, the magnitude of which is correlated very well with the acceptor strength. Figure 3 shows the V_{oc}−LUMO

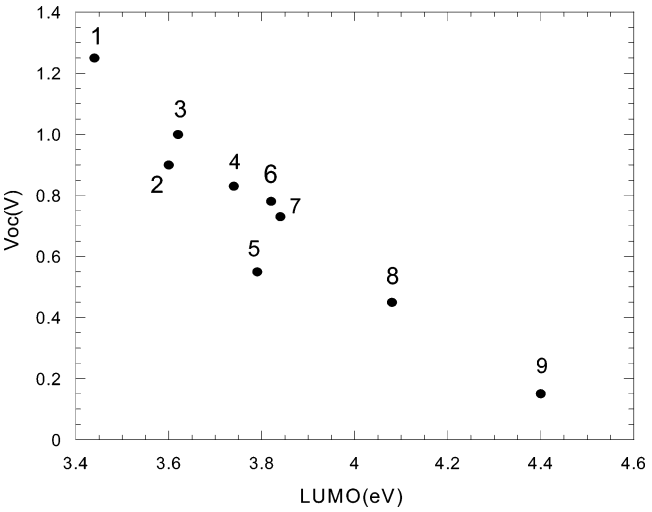

Figure 3. V_{oc} of devices from MEHPPV blend vs LUMO level of organic molecule: (0) MEHPPV, (1) MEHPPV:DBBQ, (2) MEHPPV:PF-OX, (3) MEHPPV:DTABQ, (4) MEHPPV:TTBDPQ, (5) MEHPPV:TCBZ, (6) MEHPPV:DHAQ, (7) MEHPPV:C_{60}, (8) MEHPPV:DCBQ, (9) MEHPPV:TCBQ.

correlation for the devices under illumination of white light (10 mW/cm^2). The V_{oc} decreases linearly with increasing LUMO levels of acceptors in the test range of almost 1 eV (between 3.4 and 4.4 eV). Data in Figure 3 indicate that the V_{oc} in the

TABLE 2: Devices Characteristics with Pure MEH−PPV and MEH−PPV Blended with Organic Molecule(Weight ratio of acceptor to MEHPPV equal 1:3)

	illumination under 10 mW/cm^2			at 0 bias, 550 nm	
active layer	*Voc* (V)	*Isc* (mA/cm^2)	*FF* (%)	η_e (%)	photosensitivity (A/Watt)
MEHPPV	1.50	0.00360	32.1	0.0034	0.00012
MEHPPV + DBBQ(1)	1.25	0.02340	22.6	0.0280	0.00100
MEHPPV + PF-OX(2)	0.90	0.01980	30.6	0.0250	0.00090
MEHPPV + DTABQ(3)	1.00	0.00372	37.1	0.0070	0.00019
MEHPPV + TTBDPQ(4)	0.83	0.00246	14.3	0.0028	0.00024
MEHPPV + TCBZ (5)	0.55	0.00564	30.9	0.0059	0.00035
MEHPPV + DHAQ(6)	0.78	0.00462	33.3	0.0051	0.00020
MEHPPV + C60(7)	0.73	1.44000	40.1	1.3400	0.04600
MEHPPV + DCBQ (8)	0.45	0.00288	38.9	0.0059	0.00034
MEHPPV + TCBQ(9)	0.15	0.00498	29.7	0.0013	0.00028

TABLE 3: Devices Characteristics with Pure MEHPPV and MEHPPV Blended with Organic Molecule (Weight Ratio of Acceptor to MEHPPV Equals 1:3)

	illumination under 10 mW/cm^2			at 0 bias, 550 nm	
active layer	*Voc* (V)	*Isc* (mA/cm^2)	*FF* (%)	η_e (%)	photosensitivity (A/Watt)
MEHPPV	1.50	0.0036	32.1	0.0034	0.00012
MEHPPV/DHAQ	0.78	0.0046	33.3	0.0051	0.00020
MEHPPV/DCHAQ	0.80	0.0072	35.7	0.0134	0.00047

blend devices is determined by the difference between the work function of PEDT-PSS (4.8 eV)[26] and LUMO level of acceptor. The Fermi-level pinning at LUMO of acceptor phase and its relation with V_{oc} was first discussed by Santa Barbara group through energy level analysis[4] and confirmed in a series of MDMO-PPV/C60 derivative systems over ~0.2 eV range at LUMO near 4.0 eV.[10] The data demonstrated in Figure 3 confirm that this relation is valid (1) over much broader energy ranges (nearly 1 eV demonstrated in this study) and (2) more generally with other type of organic acceptors.

Table 2 lists the device performances from MEHPPV blend with a variety of organic acceptors. Device from MEHPPV/C_{60} was included for comparison. In Table 2, the quantum efficiency (defined as Isc/Pin) was calculated as the following:

$$\text{IPCE\%} = \frac{\#\text{ electrons}}{\#\text{ photons}} \times 100 = 124000 \times \frac{I_{sc}}{P_{in}\lambda} = \frac{124000 P_S}{\lambda}$$

where I_{sc} is the short-circuit current (A/cm^2), P_{in} is the incident light power (W/cm^2), P_S is the photosensitivity (A/W), and λ is the wavelength (nm). The photosensitivity and IPCE are relatively low for all the devices made with the small molecule acceptors used in this study, much lower than devices with C_{60} as acceptors. This fact is in great contrast to the significant V_{oc} reduction and PL quenching shown in Table 1. Two possible causes may be responsible for this fact: (1) poor compatibility between nonpolar MEHPPV and highly polar organic acceptors; (2) low mobility of such organic acceptors, because of shorter π-conjugation than that in C_{60}. To better address the cause, additional experiments were designed as follows.

In the previous work, we have shown that longer alkyl chain attached to PCBM could improve significantly the compatibility of C_{60} derivatives and MEHPPV.[27] Following the same strategy, one of the selected small molecular acceptors (1, 2-dihydroxyanthraquinone, DHAQ) was modified by substitution with a long alkoxy chain (decanoxy), which results in a new compound (1,2-decanoxyanthraquinone, DCHAQ). Better compatibility with MEHPPV is anticipated. The molecule structure of DCHAQ is also shown in Figure 1. The LUMO level of DHAQ is the closest to that of C_{60} in the organic acceptors shown Table 1. Figure 4 compares the photosensitivity−wavelength response

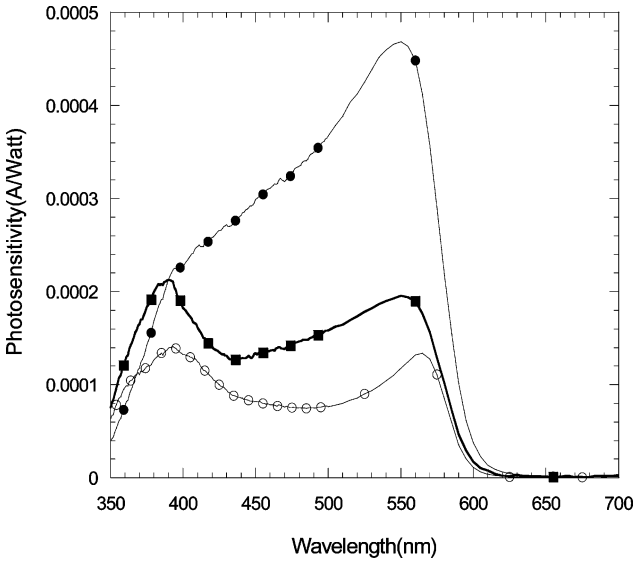

Figure 4. Photosensitivity of devices at 0 bias voltage:MEHPPV: DCHAQ (solid circle), MEHPPV:DHAQ (solid square), MEHPPV (dashed circle).

of the devices made with MEHPPV and its blends with DHAQ and DCHAQ. They were measured at 0 bias. The photosensitivity in device of MEHPPV:DHAQ increased by a factor of 2 more than in device of pure MEHPPV. By replacing DHAQ with DCHAQ in the same weight ratio, the photosensitivity was improved further by another factor of 2. Table 3 summarizes the performance of the devices fabricated under the same condition and tested under illumination of white light (10 mW/cm^2). The open-circuit voltage remains almost the same (ca. 0.8 V) for devices with DHAQ or DCHAQ in the MEHPPV blend, the same number as obtained from MEHPPV:C_{60} blend. This fact indicates that photoinduced charge generation and subsequent charge separation occurs in all these blend systems. Since the LUMO level was unchanged essentially after modification [LUMO (DCHAQ) = 3.80 eV, while LUMO (DHAQ) = 3.82 eV], we attribute the improved photosensitivity/IPCE

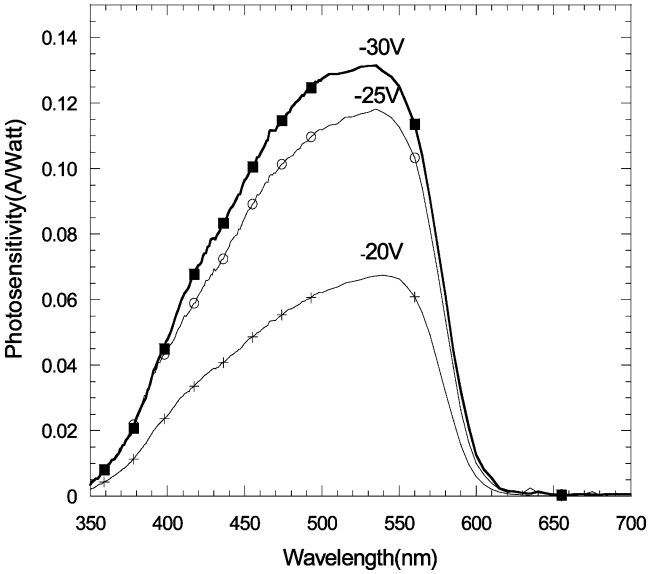

Figure 5. Photosensitivity of MEHPPV/DCHAQ devices at different biasing voltage (solid squares: −30 V, dashed circles: −25 V, and crosses: −20 V).

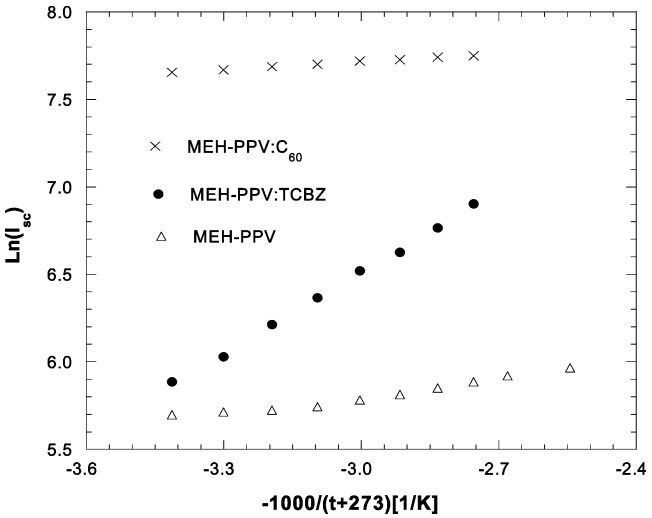

Figure 6. Photocurrent to temperature of photodiodes made with MEHPPV blended with C_{60} and TCBZ and pure MEHPPV (cross: MEHPPV:C_{60}, solid circle: MEHPPV:TCBZ; dashed triangle: MEHPPV).

in MEHPPV:DCHAQ blend to the improved donor/acceptor compatibility.

Another important fact is that the photosensitivity of MEHPPV:DCHAQ devices increases remarkably with the reverse bias. Figure 5 compares the photosensitivity of MEHPPV:DCHAQ device at different biasing voltages. Under −30 V, the maximum photosensitivity (at 540 nm) increased by more than 300 times in comparison with that at 0 V bias and reached 0.14 A/W with IPCE of 33% el/ph which is almost the same as the best MEHPPV/PCBM device at zero bias voltage. The dark current of these devices is very low, $\sim 10^{-11}$ A/cm^2. These devices are thus promising to be used as photodetectors in practical application. The strong voltage dependence of photocurrent suggests a field dependent mobility. Whether it is due to the electronic structure of the acceptor molecules or due to phase structure and grain-boundary conditions of the acceptor phase need to be addressed in future.

Figure 6 compares photocurrent versus temperature for MEHPPV, MEHPPV:C_{60}, and MEHPPV:TCBZ devices. Thermally activated photocurrents were revealed for all cases, with thermal-activation energies at 0.04, 0.01, and 0.14 eV, respectively, for MEHPPV, MEHPPV:C_{60}, and MEHPPV:TCBZ. Photoresponse of MEHPPV:TCBZ devices shows the strongest activation behavior while that of MEHPPV:C_{60} devices shows the least. Moreover, at 120 °C, the photocurrent in the MEHPPV:TCBZ device rises substantially to near the level of MEHPPV:C_{60} devices. Since TCBZ has almost the same LUMO level as C_{60}, the cause of different activation energy for these devices may be more related with morphology and phase behavior than the LUMO level of the acceptors. Again, the temperature dependence of photocurrent and IPCE could be explained by trapping conduction in acceptor phase. Whether it is due to intrinsic electronic structure of TCBZ molecules or due to phase structure and grain boundary of TCBZ aggregates are to be addressed in the future.

IV. Conclusions

In summary, we have studied characteristics of polymer PVCs on the basis of composite films of MEHPPV and a series of organic acceptors with LUMO level spread in range of 1 eV around LUMO level of C_{60}. The results demonstrated that the V_{oc} decreases linearly with increasing LUMO levels of acceptors in the test LUMO range over 1 eV and that both the interfacial properties of two phases (donor and acceptor) and the mobility of electron and the holes within corresponding phases are important for the efficiencies of PV cells. The photoelectronic conversion of the devices can be several times improved by modifying the structure of the selected small molecule as an acceptor because of improvement in compatibility of D/A phases. A strong electric field and a temperature dependence of photocurrent in the composite devices was also observed and discussed. For MEHPPV/DCHAQ device at −30 V, the maximum photosensitivity (at 540 nm) reached 0.14 A/W with IPCE of 33% as high as the best MEHPPV:PCBM devices at 0 bias. Photocurrent at 120 °C for MEHPPV:TCBZ devices increased to the level close to that of the MEHPPV:C_{60} devices at room temperature. From these results, we tentatively conclude that the mobility of the acceptor phase other than phase compatibility is a limiting factor in device performance in such a system.

Acknowledgment. The work was partially supported by the NSFC project (#50028302) and the Science Foundation of Guangdong Province (#990623) and MOST Project (#2002CB613404).

References and Notes

(1) Yu, G.; Zhang, C.; Heeger, A. J. *Appl. Phys. Lett.* **1994**, *64*(12), 1540.

(2) Yu, G.; Pakbaz, K.; Heeger, A. J. *Appl. Phys. Lett.* **1994**, *64*(25), 3422.

(3) Tani, T.; Grant, P. M.; Gill, W. D.; Street, G. B.; Clarke, T. C. *Solid State Commun.* **1980**, *33*, 499.

(4) Yu, G.; Heeger, A. J. *J. Appl. Phys*. **1995**, *78*, 4510.

(5) Sariciftci, N. S.; Smilowitz, L.; Heeger, A. J.; Wudl, F. *Science* **1992**, *258*, 1474. Sariciftci, N. S.; Heeger, A. J. U.S. Patent 5,333,183, July 19, 1994. Sariciftci, N. S.; Heeger, A. J. U.S. Patent 5,45880, Oct. 3, 1995.

(6) Kanicki, J. In *Handbook of Conducting Polymers*, Skotheim, T. A., Ed.; Marcel Dekker: New York, 1986; p 543.

(7) Antoniadis, H.; Hsieh, B. R.; Abkowitz, M. A.; Jenekhe, S. A.; Stolka, M. *Synth. Met.* **1994**, *64*, 265.

(8) Sariciftci, N. S.; Braun, D.; Zhang, C.; Srdanov, V.; Heeger, A. J.; Stucky, G.; Wudl, F. *Appl. Phys. Lett.* **1993**, *51*, 85.

(9) Lee, C. H.; Yu, G.; Moses, D.; Pakbal, K.; Zhang, C.; Sariciftci, N. S.; Heeger, A. J.; Wudl, F. *Phys. Rev. B.* **1993**, *48*, 15425.

(10) Brabec, C. J.; Cravino, A.; Meissner, D.; Sariciftci, N. S.; Fromherz, T.; Rispens, M. Y.; Sanchez, L.; Hummelen, J. C. *Adv. Funct. Mater*. **2001**, *11*, 374.

(11) Yu, G.; Gao, J.; Yang, C. Y.; Heeger, A. J. In *Proceedings of SPIE Photodetectors: Materials and Devices*; Brown, G. J., Razeghi, M., Eds.; SPIE-The International Society for Optical Engineering: Bellingham, WA, 1997; Vol. 2999, p 306.

(12) Yu, G.; Gao, J.; Hummelen, J. C.; Wudl, F.; Heeger, A. J. *Science* **1995**, *270*, 1789.

(13) Yu, G.; Srdanov, G.; Wang, H.; Cao, Y.; Heeger, A. J. *Organic Photovoltaics*; Kafafi, Z. H., Ed.; Proceedings of SPIE; SPIE-The International Society for Optical Engineering: Bellingham, WA, 2001; Vol. 4108, p 48.

(14) Deng, X. Y.; Zheng, L. P.; Mo, Y. Q.; Yu, G.; Yang, W.; Weng, W. H.; Cao, Y. *Chin. J. Polym. Sci.* **2001**, *19*, 597.

(15) Brabec, C. J.; Shaheen, S. E.; Winder, C.; Sariciftci, N. S.; Denk, P. *Appl. Phys. Lett.* **2002**, *80*, 1288.

(16) Zhang, F. L.; Johansson, M.; Mats, R. A.; Jan, C. H.; Olle, I. *Adv. Mater*. **2002**, *14*(9), 662.

(17) Svensson, M.; Zhang, F.; Veenstra, S. C.; Verhees, W. J. H.; Hummelen, J. C.; Kroon, J. M.; Inganäs, O.; Andersson, M. R. *Adv. Mater*. **2003**, *15*, 988.

(18) Brabec, C. J.; Winder, C.; Sariciftci, Hummelen, J. C.; Dhanabalan, A.; van Jassen, A. J. *Adv. Funct. Mater*. **2001**, *11*, 709.

(19) Schmidt-Mende, L.; Fechtenkötter, A.; Müllen, K.; Moons, E.; Friend, R. H.; MacKenzie, J. D. *Science* **2001**, *293*, 1119.

(20) Shaheen, S. E.; Brabec, C. J.; Sarciftci, N. S.; Padinger, F.; Fromherz, T.; Hummelen, J. C. *Appl. Phys. Lett*. **2001**, *78*, 841.

(21) Morgado, J.; Cacialli, F.; Friend, R. H.; Iqbal, R.; Yahiglu, G.; Milgrom, L. R.; Morratti, S. C.; Holmes, A. B. *Chem. Phys. Lett.* **2000**, *325*, 552.

(22) Wang H.; Yu, G.; Srdanov, G. PCT application, WO 2001077203 A2, 11 Apr. 2000.

(23) Wudl, F.; Allemand, P. M.; Srdanov, G.; Ni, Z.; McBranch, D. In *Materials for Nonlinear Optics: Chemical Perspectives*; Marder, S. R., Sohn, J. E., Stucky, G. D., Eds.; The American Chemical Society: Washington, DC, 1991; 163.

(24) Leeuw, D. M.; Simenon, M. M. J.; Brown, A. R.; Einerhand, R. E. F. *Synth. Met.* **1997**, *87*, 53.

(25) Ramsdale, C. M.; Barker, J. A.; Arias, A. C.; MacKenzie, J. D.; Friend, R. H.; Greenham, N. C. *Appl. Phys. Lett.* **2002**, *92*, 4266.

(26) Cao, Y.; Yu, G.; Zhang, C.; Menon, R.; Heeger, A. J. *Synth. Met.* **1997**, *87*, 171.

(27) Zheng, L. P.; Zhou, Q. M.; Deng, X. Y.; Yuan, M.; Yu, G.; Cao, Y. *Synth. Met*. **2003**, *135*, 827.